

Universal properties of correlation transfer in integrate-and-fire neurons

Eric Shea-Brown,^{1,2} Krešimir Josić,³ Jaime de la Rocha,² and Brent Doiron^{1,2}

¹*Courant Institute of Mathematical Sciences, New York University, New York, NY 10012*

²*Center for Neural Science, New York University, New York, NY 10012*

³*Department of Mathematics, University of Houston, Houston, TX 77204-3008*

(Dated: November 20, 2018)

One of the fundamental characteristics of a nonlinear system is how it transfers correlations in its inputs to correlations in its outputs. This is particularly important in the nervous system, where correlations between spiking neurons are prominent. Using linear response and asymptotic methods for pairs of unconnected integrate-and-fire (IF) neurons receiving white noise inputs, we show that this correlation transfer depends on the output spike firing rate in a strong, stereotyped manner, and is, surprisingly, almost independent of the interspike variance. For cells receiving heterogeneous inputs, we further show that correlation increases with the geometric mean spiking rate in the same stereotyped manner, greatly extending the generality of this relationship. We present an immediate consequence of this relationship for population coding via tuning curves.

Systems with spatially correlated, stochastic forcing provide a rich field of study, with applications ranging from polymer physics to population biology [1]. In neuroscience, much theoretical work focusses on correlation (or synchrony) between *coupled* neurons receiving uncorrelated external fluctuations [2]. Nevertheless, in sensory systems, external fluctuating signals common to a group of unconnected cells [3, 15] are a strong source of correlations. Moreover, signal-independent correlations can develop within strictly feedforward networks, due to convergent connections between layers [4, 14]. Furthermore, the connectivity within biological neural networks is often sparse [5], suggesting that pairs of neurons rarely influence one another directly [12]. These observations have prompted experimental and theoretical efforts [6, 7, 9] to characterize the transfer of correlated input currents to correlated spikes for pairs of *uncoupled* neurons. Despite the straightforward setting of this problem, few common principles have emerged.

Recently, we have observed that in response to fluctuating input currents with *fixed* levels of correlation, the spike (output) correlation between pairs of neurons increases with the spiking rate and was approximately independent of the spiking variance [13]. We provided empirical evidence for this correlation-rate relationship in *in vitro* cortical data and in IF models with ‘hard’ thresholds, for homogeneous cell pairs firing at low to medium rates. In this letter, we develop an analytical approach that both explains and greatly extends these observations. Specifically, we obtain closed-form expressions relating output correlations to firing (spiking) rate, show that a refractory period implies the existence of optimal firing rates for correlation transfer, and show that correlation transfer depends approximately only on the geometric mean of the output firing rates for heterogeneous cell pairs. We demonstrate extensions to the quadratic integrate and fire model and to a broader analysis of the *in vitro* data. These results enable us to develop the first consequences of the correlation-rate relationship

for cortical coding, where populations of heterogeneously tuned neurons relay information about the sensory environment.

Model – The model consists of two IF neurons receiving common $\xi(t)$ and independent $\xi_i(t)$ white noise inputs (Fig. 1a):

$$\tau V_i' = f(V_i) + \mu_i + \sigma_i \sqrt{\tau} \left[\overbrace{\sqrt{1-c} \xi_i(t) + \sqrt{c} \xi(t)}^{I_i(t)} \right], \quad (1)$$

$i = 1, 2$. Here, V_i denotes the membrane voltage of cell i , τ is the membrane time constant, and $f(\cdot)$ defines the subthreshold dynamics. We mostly take $f(V_i) = -V_i$ (leaky IF), but in one section use $f(V_i) = V_i^2$ (quadratic IF). We adopt the standard threshold-spike-reset condition: $V_i(t^+) = V_R$ whenever $V_i(t) = V_T$; at such times, a spike is emitted, after which the voltage is held at V_R during the *refractory period* τ_r . Throughout, we set $\tau = 1$ (we report rates in units of τ^{-1}). Of interest are the normalized output spike trains $y_i(t) = \sum_i \delta(t - t_i^k)$, where t_i^k is the k^{th} spike time of the i^{th} neuron. The firing rate of the i^{th} cell is $\nu_i = \langle y_i(t) \rangle$.

The input current $I_i(t)$ to cell i has a constant (DC) component μ_i as well a stochastic component with amplitude σ_i (Fig. 1a). The stochastic component to each cell is the sum of two independent gaussian processes, $\xi_i(t)$ and $\xi(t)$, with $\langle \xi_i(t) \xi_j(t') \rangle = \delta_{ij} \delta(t-t')$ and $\langle \xi_i(t) \xi(t') \rangle = 0$ ($i, j = 1, 2$); note that $\xi(t)$ is common to both cells. The weights $\sqrt{1-c}$ and \sqrt{c} result in a correlation coefficient c between $I_1(t)$ and $I_2(t)$. The spike correlation coefficient, ρ , is computed [7, 8, 10, 13] by integrating the spike auto- and cross-correlation functions $C_{ij}(\tau) = \langle y_i(t) y_j(t + \tau) \rangle - \nu_i \nu_j$:

$$\rho = \frac{\int_{-\infty}^{\infty} C_{12}(\tau) d\tau}{\sqrt{\int_{-\infty}^{\infty} C_{11}(\tau) d\tau} \sqrt{\int_{-\infty}^{\infty} C_{22}(\tau) d\tau}}. \quad (2)$$

Linear response calculations – Following methods of [15], we derive an analytic expression for ρ valid to linear order in c ; simulations of Eq. (1) verify that

these methods produce good approximations for c up to ≈ 0.3 [13], and were repeated to the same effect for the cases studied here (data not shown).

The cross spectrum of the spike trains $y_1(t)$ and $y_2(t)$ is $P_{12}(\omega) = \langle \tilde{y}_1^*(\omega)\tilde{y}_2(\omega) \rangle$, where the Fourier transform $\tilde{y}_i = \frac{1}{\sqrt{T}} \int_0^T e^{i\omega t} (y_i(t) - \nu_i) dt$. Treating the common term $\sqrt{c}\xi(t)$ as a perturbation, we use the linear approximation [15]:

$$\tilde{y}_i(\omega) = \tilde{y}_{i,\mu_i,\sigma_i\sqrt{1-c}}(\omega) + \sigma_i\sqrt{c}A_{\mu_i,\sigma_i\sqrt{1-c}}(\omega)\tilde{\xi}(\omega) + \mathcal{O}(c). \quad (3)$$

Here $\tilde{y}_{i,\mu_i,\sigma_i\sqrt{1-c}}(\omega)$ is the Fourier transform of a spike train obtained from a neuron driven only by the ‘‘private’’ input $\mu_i + \sigma_i\sqrt{1-c}\xi_i(t)$ (i.e., in the *absence* of a common stochastic input), and $A_{\mu_i,\sigma_i\sqrt{1-c}}(\omega)$ is the susceptibility function of such a neuron [23].

Inserting Eq. (3) into the definition of the cross spectrum we obtain:

$$P_{12}(\omega) = c\sigma_1\sigma_2A_{\mu_1,\sigma_1}^*(\omega)A_{\mu_2,\sigma_2}(\omega)P_\xi(\omega) + \mathcal{O}(c^{3/2}) \quad (4)$$

where $P_\xi(\omega) = \langle \tilde{\xi}^*(\omega)\tilde{\xi}(\omega) \rangle = 1$. Here we used $\langle \tilde{y}_{i,\mu_i,\sigma_i\sqrt{1-c}}^*\tilde{y}_{j,\mu_j,\sigma_j\sqrt{1-c}} \rangle = \langle \tilde{y}_{i,\mu_i,\sigma_i\sqrt{1-c}}^*\tilde{\xi} \rangle = 0$, $i, j = 1, 2$. We also used the fact that the $\mathcal{O}(c)$ terms in Eq. (3) arise from ξ , so are statistically independent of the $\tilde{y}_{i,\mu_i,\sigma_i\sqrt{1-c}}$. Moreover, we evaluate the susceptibility terms at $c = 0$, which is valid to the order of error shown.

The Wiener-Khinchine Theorem yields $P_{12}(0) = \int_{-\infty}^{\infty} C_{12}(t)dt$; also, the susceptibility to DC input is $A_{\mu_i,\sigma_i}(0) = \frac{d\nu_i}{d\mu_i}$. Thus, substituting Eq. (4) into Eq. (2) yields to lowest order in c :

$$\rho = c\sigma_1\sigma_2 \frac{\frac{d\nu_1}{d\mu_1} \frac{d\nu_2}{d\mu_2}}{CV_1 CV_2 \sqrt{\nu_1 \nu_2}}, \quad (5)$$

where we have additionally used the result for renewal point processes $\int_{-\infty}^{\infty} C_{ii}(\tau)d\tau = CV_i^2\nu_i$; here, CV_i is the coefficient of variation of the inter-spike interval distribution [19].

Dependence of correlations on firing rate. – We first assume that the statistics of inputs to cells i and j are identical ($\mu_i = \mu_j \equiv \mu$ and $\sigma_i = \sigma_j \equiv \sigma$), giving

$$\rho = c\sigma^2 \left(\frac{d\nu}{d\mu} \right)^2 \triangleq cS(\mu, \sigma). \quad (6)$$

Here S is the **correlation susceptibility** [13] between the input current correlation c and the spike (output) correlation ρ .

We explain three key features of Eq. (6): *i*) S increases with firing rate ν for low to moderate rates. *ii*) S is approximately a function of ν *alone*, independent of the precise values of μ and σ or the CV. At low rates this relationship becomes exact. *iii*) For large rates: S tends to a constant near 1 if $\tau_r = 0$ and tends to zero if $\tau_r > 0$.

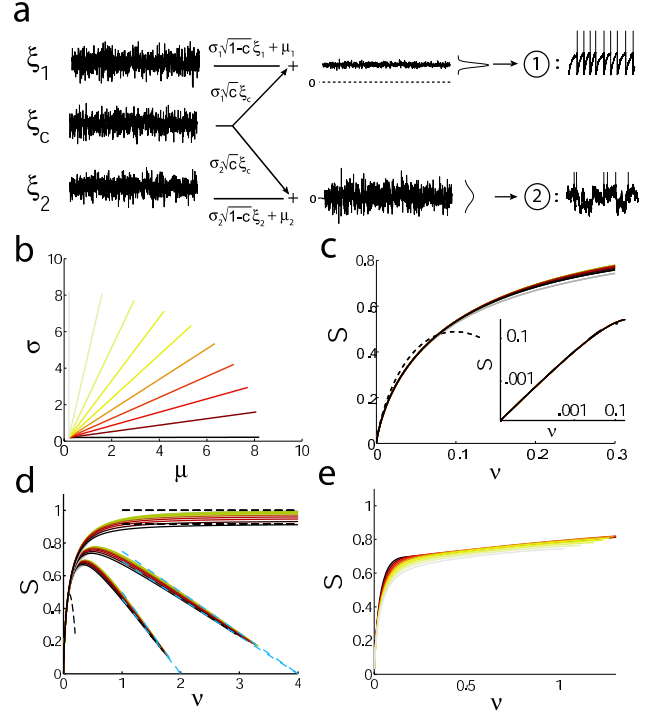


FIG. 1: a) Schematic of two cells receiving heterogeneous, correlated white noise inputs. b) Rays with different $\beta = \mu/\sigma$; grayscale (color online) applies to the following panels. c) S vs. ν increasing along the different rays for a limited range of rates for LIF cells, $\tau_r = 0$. Here and for all figures with LIF model: $V_T = 1$, $V_R = 0$. Kramer’s approximation shown as dotted line. Inset, on log-log axes. d) As (c), for wider range of rates. Dotted lines show Kramer’s approximation at low rates and large μ , σ approximations at high rates. Sets of curves, from top to bottom: $\tau_r = 0$, $\tau_r = 0.25$, $\tau_r = 0.5$. e) Similar, but for QIF model with $\tau_r = 0$, $V_T = 10$, $V_R = -10$.

To study the low rate case we treat the voltage of each cell as a particle in the potential $\phi(V) = (V - \mu)^2/2$. Low rates are obtained only when $\mu < V_T$ and $0 < \sigma \ll 1$. In this limit, Kramer’s theory can be applied to calculate the terms in S , by computing the mean (m) and the variance (var) of hitting times of the threshold voltage V_T for particles starting at the bottom of the wells, and by noting that $\nu = (m + \tau_r)^{-1}$ and $CV^2 = \nu^2 \text{var}$. Asymptotic results [16] give, to lowest order in σ ,

$$\nu = \frac{\alpha}{\sqrt{\pi}} \exp(-\alpha^2) \triangleq g(\alpha), \quad (7)$$

and $\frac{d\nu}{d\mu} = \frac{\nu}{\sigma} (2\alpha - \frac{1}{\alpha})$, where $\alpha = \frac{V_T - \mu}{\sigma}$. Moreover, $CV^2 = 1$ to lowest order in σ , as the threshold crossing times are exponentially distributed in this limit. Therefore, here we have $S \approx \nu(2\alpha - 1/\alpha)^2$. Eq. (7) may be uniquely inverted for a range of sufficiently small σ (large α) to yield $\alpha = g^{-1}(\nu)$. For small ν we obtain:

$$S(\mu, \sigma) \approx \hat{S}(\nu) = \nu \left(2g^{-1}(\nu) - \frac{1}{g^{-1}(\nu)} \right)^2, \quad (8)$$

so that asymptotically S is a function of ν *alone* (Fig. 1c).

Asymptotics for large firing rate ν are obtained from exact expressions for the firing rate and variance [20]. Using asymptotic approximations, we obtain for fixed σ and large μ

$$S(\mu, \sigma) \approx \frac{(V_T - V_R)}{\mu\tau_r + (V_T - V_R)}.$$

Thus, the correlation susceptibility S approaches 0 in the large μ limit, as long as $\tau_r > 0$. In the case $\tau_r = 0$, we obtain $S \rightarrow 1$ as $\mu \rightarrow \infty$ (Fig. 1d).

More generally, if μ and σ diverge jointly so that $\mu/\sigma = \beta$ is constant (i.e., along a ray in Fig. 1b), we obtain $S(\mu = \beta\sigma, \sigma) \approx \frac{K_1(\beta)(V_T - V_R)}{K_2(\beta)(V_T - V_R) + \sigma\tau_r}$. Here, $K_1(\beta) = \frac{(-2/\sqrt{\pi} + 2\beta e^{\beta^2} \operatorname{erfc}(\beta))^2}{2e^{\beta^2} \int_{\beta}^{\infty} e^{x^2} \operatorname{erfc}^2(x) dx}$ and $K_2(\beta) = \sqrt{\pi} e^{\beta^2} \operatorname{erfc}(\beta)$. Using asymptotic expressions for ν at large μ and σ , we obtain

$$S(\mu, \sigma) \approx \hat{S}(\nu) = \frac{K_1(\beta)}{K_2(\beta)} (1 - \tau_r \nu). \quad (9)$$

The constant $K_1(\beta)/K_2(\beta)$ increases from 0.918 to 1, as β increases from 0 to ∞ . Therefore, if $\tau_r = 0$, $S(\nu)$ is asymptotic to values in the interval $[0.918, 1]$ for large ν , as shown in Fig. 1d. Furthermore, if $\tau_r \neq 0$ then $S(\nu)$ tends to zero at $\nu = \tau_r^{-1}$, with slope in $[-1, -0.918]$.

In summary, we have shown that, at low rates, S is asymptotically a function of ν *only*, regardless of specific values of σ and μ and hence of the CV. At high rates, if $\tau_r = 0$ then S is bounded in a neighborhood of 1; if $\tau_r > 0$ then S tends to zero within a narrow ‘‘cone’’ at rates near the limit $\nu = \tau_r^{-1}$. It follows that a refractory period implies that S obtains a maximum at a particular firing rate, at which the neuron is ‘‘best-tuned’’ to transfer input correlations to output correlations. For intermediate rates, numerical evaluations of Eq. (6) show that S remains an approximate function of ν alone, a fact that greatly simplifies the statistical description of the LIF model. We note that these findings hold more generally: Fig. 1e shows analogous results for the quadratic integrate and fire model, demonstrating that our results depend on neither the linear subthreshold dynamics nor the ‘‘hard’’ threshold condition of the LIF model.

Effects of heterogeneity. – We return to the general Eq. (5). In neuroscience, several studies plot the output correlation of two cells versus the geometric mean of their firing rates $\sqrt{\nu_1 \nu_2}$ [8, 9, 10]. Fig. 2a shows the corresponding predictions of Eq. (5), as the input parameters $\{\mu_1, \sigma_1, \mu_2, \sigma_2\}$ are sampled over a wide range, producing very different combinations of $\nu_i, CV_i, i = 1, 2$ (here and below we take $\tau_r = 0$). Remarkably, when ρ is plotted vs. $\sqrt{\nu_1 \nu_2}$, we see approximately the *same* correlation-rate relationship as for the homogeneous case. At low rates, this relationship becomes almost independent of

the ratio $h = \nu_1/\nu_2$ ($\nu_1 > \nu_2$) between the cells’ rates; at higher rates, it depends only weakly on h . Thus, in the limit of small c we have:

$$\rho = c\sqrt{S(\mu_i, \sigma_i)S(\mu_j, \sigma_j)} \approx c\sqrt{\hat{S}(\nu_i)\hat{S}(\nu_j)} \approx c\hat{S}(\sqrt{\nu_i \nu_j}). \quad (10)$$

Here, the first approximation follows from our results for the homogenous case, and the second follows empirically from Fig. 2a.

To see how surprising this is, consider the four voltage traces in Fig. 2a, each of which displays either a high or low CV, and a high or low rate ($\nu = 0.47$ or 0.047 , resp.). Nevertheless, any combination of these cases that gives the *same* geometric mean (AB, AC, BD, CD, $\sqrt{\nu_1 \nu_2} = 0.15$) gives the *same* value of $S = 0.55$, within less than 1% (square on graph). This is despite the strongly distinct structure of the correlation functions for these different pairings (AB, CD shown). Other striking predictions similarly follow from Eq. (10): for example, simply adding a DC current to one of a pair of cells (thus increasing, e.g., ν_i) should increase their spike correlation.

Why does Eq. (10) hold? Fig. 1 shows that $S(\mu_i, \sigma_i) \approx \hat{S}(\nu_i)$, with exact agreement at low rates. The approximation $\sqrt{\hat{S}(\nu_i)\hat{S}(\nu_j)} \approx \hat{S}(\sqrt{\nu_i \nu_j})$ would be exact if $\hat{S}(\nu_i)$ was a power law, $\hat{S}(\nu_i) \propto \nu_i^\gamma$, and Fig. 1c (inset) shows that this is an excellent approximation at low rates. Hence Eq. (10) holds precisely at low rates, so that the different areas in Fig. 2a converge. To explore when the approximation $\sqrt{\hat{S}(\nu_i)\hat{S}(\nu_j)} \approx \hat{S}(\sqrt{\nu_i \nu_j})$ breaks down, we study the special case where the ratio $\beta_i = \sigma_i/\mu_i = 1$ is identical for both cells (Fig. 2b). Fig. 2c shows level sets of this surface on log-log axes (thick lines), which almost superpose with level sets of $\sqrt{\nu_i \nu_j}$ (thin black lines) for low rates, or for values of h reasonably close to 1 (shaded areas). For larger rates, or greater heterogeneity, these level sets start to diverge. However, even then the disagreement is quite mild: for h up to 10, values of S along level sets of $\sqrt{\nu_i \nu_j}$ do not vary by more than $\approx 10\%$, because S varies only weakly with large rates. This agreement stands in contrast to that between level sets of S and of the arithmetic mean $(\nu_1 + \nu_2)/2$, shown as grey lines (red online), indicating that the choice of the geometric mean is somewhat special in capturing the rate-dependence of S . Fig. 2d shows that this relationship holds not only for the LIF model, but also for our *in vitro* experiments. Here, pairs of cortical cells in mouse brain slices were injected with correlated, noisy, low-pass filtered currents, replicating the configuration of Fig. 1a (see [13] for experimental methods). Output spikes were recorded via whole-cell patch clamp, and ρ was computed from paired spike trains as described above.

For an illustration of the functional consequences of the rate-correlation relationship for heterogeneous cells, con-

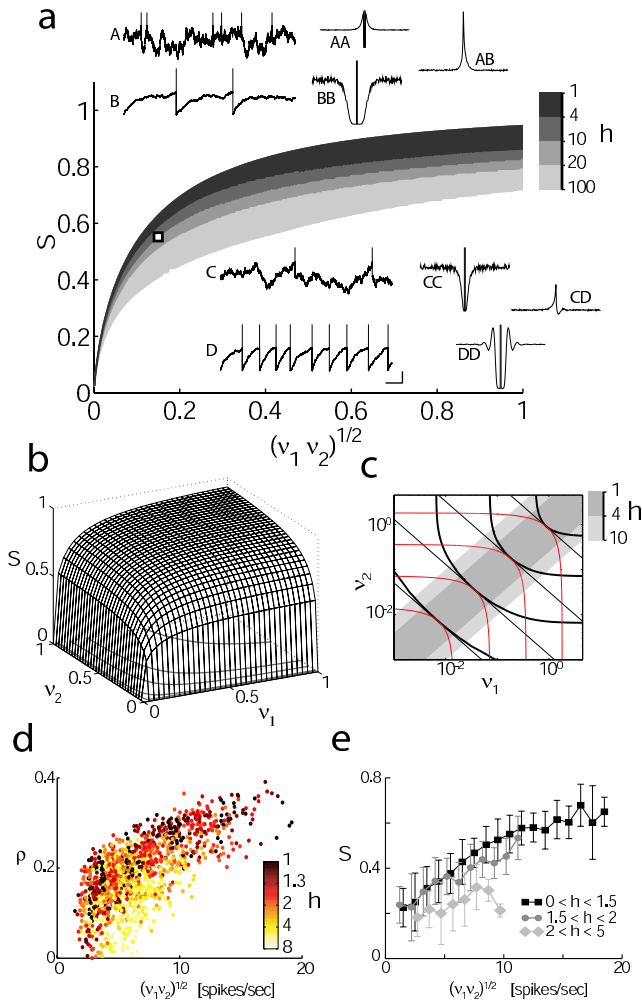


FIG. 2: (a) S vs. $\sqrt{\nu_1 \nu_2}$, from Eq. (5). Input parameters $\{\mu_1, \sigma_1, \mu_2, \sigma_2\}$ were sampled over a 4-D cube ($\mu_{i,j} \in [2, 8.2]$, $\sigma_{i,j} \in [2, 8.2]$, grid spacing 0.01-0.05, with denser grid for $\mu, \sigma < 1.6, 2.2$). Overlapping regions shaded from dark to light contain all points with levels of $h = \nu_1/\nu_2$ varying over increasingly broad ranges. Square marks value for the pairings AB, AC, BD, CD shown in the inset (voltage traces and auto- and cross-correlation functions plotted); see text. Horizontal scale bar: 2τ for voltage traces, 4τ for correlation functions. Vertical scale bar: .25 for correlation functions, .5 for traces B, D, 1 for traces A, C. (b) Surface/contour plot of S , where $\sigma = \mu$ for both cells. (c) Contour plot on log-log axes; see text. (d, e) S vs. $\sqrt{\nu_1 \nu_2}$ for *in vitro* cortical experiments; (d), raw data 1269 pairwise comparisons obtained from 20 cells using $c = 0.5$, (e), population average and standard deviation to show trends.

consider a population of neurons whose rates ν_i are tuned to a sensory variable θ as in Fig. 3a [17, 21]. The correlation ρ_{ij} between pairs of these cells approximately depends on their geometric mean rate $\sqrt{\nu_1 \nu_2}$ according to Eq. (10), producing the correlation tuning shown in Fig. 3b (input correlations are taken to be constant: $c_{ij} \equiv c$). Thus, the fact that only neurons with similar tuning display substantial correlation, as in empirical [10, 11] and theoretic-

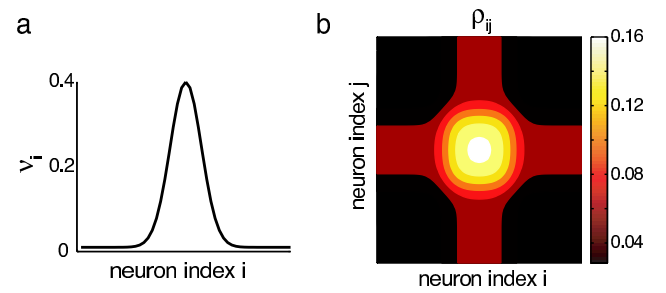


FIG. 3: (a) Firing rate in response to a given stimulus for a population of neurons with tuning curves evenly distributed across the stimulus (θ) space. (b) The resulting crosscorrelations ρ_{ij} for this stimulus, from Eq. (5).

cal [17] studies, follows directly from our results, without requiring a separate assumption that the input correlation is itself tuned. We also predict stronger correlations for neurons with “preferred” tuning to a stimulus, as in [10]. Such an extension of stimulus selectivity from rate [21] to correlation tuning has broad and novel implications for information *encoding* in spiking neurons. Further, correlations in output spike trains are effective in propagating activity downstream [4], thereby facilitating the *decoding* of correlation-based information.

Our methods can be extended: Eq. (5) holds for any cell or cell model producing spikes as a renewal process, and the preceding forms of this expression are valid even for nonrenewal spiking (enabling, e.g., analysis of temporally correlated inputs [7]). Moreover, our formulas and their reduction to a compact correlation-rate relationship may be a critical component for mean field models of sparsely coupled neural populations, where treatment of second-order statistics has previously been restricted to spike train variance (e.g., [22]). A mean field framework that rigorously includes correlations would connect neural population dynamics [2, 4, 22] with the emerging role for correlations in sensory coding.

We acknowledge Steve Coombes and Dan Tranchina for their critical reading and helpful comments, and the support of a BWF Career Award and NSF MSPRF (ESB), grants DMS-0604229 and Texas ARP/ATP (KJ), HSPF (BD), and the Spanish MEC (JR).

- [1] J. García-Ojalvo and J. Sancho. Noise in Spatially Extended Systems. Springer-Verlag, 1999; E. Medina et al. Phys. Rev. A **39** 3053, 1989; A. Liebhold, W.D. Koenig, and O.N. Bjørnstad, Annu. Rev. Ecol. Evol. Syst. **35** 347, 2004.
- [2] Y. Kuramoto. Physica D **50**, 15, 1991; S. Strogatz and R. Mirollo. J. Stat. Phys. **63** 613, 1991; L. Abott and C. Vanreeswijk. Phys. Rev. E, **48** 1483, 1993.
- [3] J. Benda, A. Longtin, and L. Maler. Neuron **52** 347, 2006; E. Schneidman et al. Nature **440** 20, 2006.

- [4] H. Cateau and A. Reyes. Phys. Rev. Lett. **96** 058101, 2006; B. Doiron, J. Rinzel, and A. Reyes. Phys. Rev. E **74** 030903, 2006; S. Wang, W. Wang, and F. Liu. Phys. Rev. Lett. **96** 108103, 2006. M. Abeles, *Corticonics*, Cambridge, 1991.
- [5] B. Hellwig. Biol. Cybern. **82** 111, 2000.
- [6] J. Dorn and D. Ringach. J. Neurophys. **89** 2271, 2003; R. Galan et al. J. Neurosci. **26** 3646, 2006; G. Svirskis and J. Hounsgaard. Network **14** 747, 2003.
- [7] R. Moreno-Bote and N. Parga. Phys. Rev. Lett. **94** 088103, 2005.
- [8] W. Bair, E. Zohary, and W. Newsome. J. Neurosci. **21** 1676, 2001.
- [9] M. Binder and R. Powers. J Neurophys. **86** 2266, 2001.
- [10] A. Kohn and M. Smith; J. Neurosci. **25** 3661, 2005;
- [11] E. Zohary, M. Shadlen, and W. Newsome. Nature **370** 140, 1994.
- [12] J. Shlens et al. J. Neurosci. **26** 8254, 2006.
- [13] J. de la Rocha, B. Doiron et al. Submitted, 2006.
- [14] M. N. Shadlen and W. T. Newsome. J. Neurosci. **18** 3870, 1998.
- [15] B. Doiron et al. Phys. Rev. Lett. **96** 048101, 2004; B. Lindner, B. Doiron, and A. Longtin. Phys. Rev. E **72** 061919, 2005.
- [16] C. Bender and S. Orszag. *Advanced mathematical methods for scientists and engineers*. Springer-Verlag, 1999.
- [17] L. Abbott and P. Dayan. Neural Comp. **11** 91, 1999; M. Shamir and H. Sompolinsky. Neural Comp. **16** 1105, 2004.
- [18] Milton Abramowitz and Irene A. Stegun. *Handbook of Mathematical Functions*. Dover, 1964.
- [19] D.R. Cox and P.A.W. Lewis. *The Statistical Analysis of a Series of Events*. Jonh Wiley, 1966.
- [20] B. Lindner. *Dissertation, Humboldt Univ. Berlin*, 2001.
- [21] D. Hubel and T. Wiesel. J. Physiol. **160** 154, 1962.
- [22] A. Renart et al, Neural Comp. **19** 1, 2007; D. Amit and N. Brunel, Cereb. Cortex **7** 237, 1997. D. Nykamp and D. Tranchina, J. Comp. Neurosci. **8**, 19.
- [23] H. Risken. *The Fokker-Planck equation*. Springer-Verlag, 1989.